

# RSC Advances



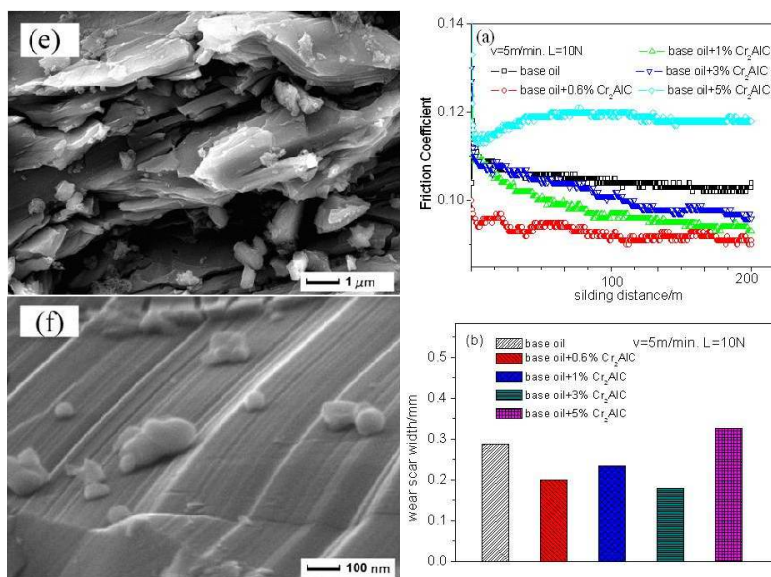
This is an *Accepted Manuscript*, which has been through the Royal Society of Chemistry peer review process and has been accepted for publication.

*Accepted Manuscripts* are published online shortly after acceptance, before technical editing, formatting and proof reading. Using this free service, authors can make their results available to the community, in citable form, before we publish the edited article. This *Accepted Manuscript* will be replaced by the edited, formatted and paginated article as soon as this is available.

You can find more information about *Accepted Manuscripts* in the [Information for Authors](#).

Please note that technical editing may introduce minor changes to the text and/or graphics, which may alter content. The journal's standard [Terms & Conditions](#) and the [Ethical guidelines](#) still apply. In no event shall the Royal Society of Chemistry be held responsible for any errors or omissions in this *Accepted Manuscript* or any consequences arising from the use of any information it contains.

## Graphical abstract

high purity  $\text{Cr}_2\text{AlC}$  nanolamellas and tribological properties for oil-based additives

Cite this: DOI: 10.1039/c0xx00000x

www.rsc.org/xxxxxx

ARTICLE TYPE

# Synthesis of high purity Cr<sub>2</sub>AlC nanolamellas with improved tribological properties for oil-based additives

Maoquan Xue<sup>a,b</sup>, Xianghua Zhang<sup>a</sup>, Hua Tang<sup>a</sup> and Changsheng Li<sup>\*a</sup>

Received (in XXX, XXX) Xth XXXXXXXXX 20XX, Accepted Xth XXXXXXXXX 20XX

DOI: 10.1039/b000000x

Herein, a novel simple method is presented to synthesize highly pure Cr<sub>2</sub>AlC powder by heating 2Cr/xAl/C (molar ratio, x=1,1.1,1.2) powder system between 1300 °C and 1400 °C with preliminary magnetic stirring mixing in alcohol. The purity of Cr<sub>2</sub>AlC is sensitive to the final temperature and raw material scale, the excess Al play a distinct role in improving the purity of Cr<sub>2</sub>AlC. The tribological properties of Cr<sub>2</sub>AlC as an additive in 100SN base oil were evaluated by a UMT-2 ball-on-disc friction and wear tester. The results show that under determinate conditions, the base oil containing 0.6wt.% Cr<sub>2</sub>AlC samples presented good tribology performance under the load of 10 N. The improved tribological properties of the Cr<sub>2</sub>AlC samples could be attributed to the formation of tribofilm in friction process.

## 1. Introduction

Chromium aluminum carbides, Cr<sub>2</sub>AlC, belong to a special group of the materials known as layered ternary compounds. This new class of materials features a hexagonal crystalline structure and can be represented by a general formula of M<sub>n+1</sub>AX<sub>n</sub> (MAX), where n = 1, 2, or 3, M is an early transition metal, A is an A-group element, and X is carbon or nitrogen,<sup>1-7</sup> the unique combination of ceramic and metallic properties has attracted considerable interest. Among them, Cr<sub>2</sub>AlC, is a member of the novel 211 ternary compounds exhibits outstanding ceramic properties such as a low density,<sup>8</sup> high melting point and thermal stability,<sup>9</sup> a low thermal expansion coefficient,<sup>10,11</sup> high strength at high temperatures,<sup>12</sup> and excellent oxidation resistance.<sup>13,14</sup> Meanwhile, Cr<sub>2</sub>AlC possesses metallic properties including relatively high electrical and thermal conductivities,<sup>15,16</sup> well resistant to thermal shock,<sup>4</sup> good damage tolerance,<sup>17,18</sup> and easy machinability.

To date, several methods including mechanically activated hot pressing,<sup>19</sup> hot isostatic pressing,<sup>20</sup> hot pressing,<sup>13,21</sup> spark plasma sintering,<sup>22</sup> and so on have been adopted to synthesize Cr<sub>2</sub>AlC from different mixtures with different mole ratios. These synthesis processes, however, usually require high energy ball milling and certain sintering equipment requirements, which lead to raw material easy being oxidation, energy and time consuming, complicated productive process and low production efficiency.<sup>23-27</sup> Therefore, it is still a great challenge to develop a facile and effective process to fabricate Cr<sub>2</sub>AlC with high purity. In addition,

<sup>a</sup> School of Materials Science and Engineering, Jiangsu University, Zhenjiang, Jiangsu Province, 212013, P.R.China. Fax: +86 511 8879 0268; Tel: +86 511 8879 0268; E-mail: changshengli2008@163.com

<sup>b</sup> Changzhou Institute of Light Industry Technology, Changzhou, Jiangsu Province, 213164, P.R.China

it was found that Cr<sub>2</sub>AlC has an excellent tribological property, especially at elevated temperatures.<sup>28-30</sup> The relatively low coefficient and wear rate are attributed to the amorphous or nanocrystalline tribofilms form on both contact surfaces. However, to the best of our knowledge, little work focused on the tribological properties of Cr<sub>2</sub>AlC as lubrication additive.

In this study, laminate-like Cr<sub>2</sub>AlC crystals with high purity were synthesised by pressureless sintering raw powders at 1300-1400 °C in a flowing argon atmosphere, the raw powders were directly mixed by magnetic stirring in alcohol. The tribological properties of Cr<sub>2</sub>AlC samples as additives in the 100SN base oil were also investigated.

## 2. Experimental

### 2.1 Synthesis of laminated Cr<sub>2</sub>AlC

Cr (99.0% pure, -200 mesh), Al (99.0% pure, -200 mesh), and graphite (99% pure, ~5µm) (all from Sinopharm Chemical Reagent Co. Ltd., Shanghai China) powders were used in this work. About 5g raw powders with stoichiometric molar ratio of 2Cr/xAl/C(x=1,1.1,1.2) were mixed by magnetic stirring in absolute alcohol at 70 °C. Alcohol evaporated in heating process, ~1h, alcohol evaporated completely. After being dried and sieved with 200-mesh screen, the blended powder was placed in a stainless steel mould with diameter of 25mm, the pressure was 30 MPa. Then, the cold pressing slices were loaded into corundum crucible and sintered in tube furnace. The samples were heated at a rate of 5 °C /min. in flowing argon atmosphere until the final temperatures (from 1300 to 1400 °C) were reached, at which the sintering time was 30 min. Finally samples were crushed and grinded into powder.

### 2.2 Characterisation of Cr<sub>2</sub>AlC samples

The raw blended powder was analyzed with differential scanning calorimetry (DSC) in an instruments analyzer (NETZSCH-Ger  
tebau GmbH Selb/Germany). The runs were performed in an argon atmosphere, with a 10 °C /min. temperature increase rate  
5 from room temperature up to 1300 °C. The phases of prepared  $\text{Cr}_2\text{AlC}$  ceramics powders were analyzed using a D8ADVANCE  
diffractometer and  $\text{Cu K}\alpha$  radiation in the  $2\theta$  range between 10° and 80°, operating at 40kV and 20mA,  $\lambda=0.1546\text{nm}$ ,  
10 respectively, data analysis with Jade software. The morphologies and microstructures of  $\text{Cr}_2\text{AlC}$  ceramics were determined by  
Scanning Electron Microscopy (SEM) (JEOL JXA-840A).

### 2.3 Tribological properties of laminated $\text{Cr}_2\text{AlC}$ crystals as lubrication additive

Different mass fractions of the as-prepared  $\text{Cr}_2\text{AlC}$  powder from  
15  $2\text{Cr}/1.2\text{Al}/\text{C}$  sintered at 1400°C were dispersed in 100SN base oil via 2h ultrasonication without any active reagent, and then a  
series of suspended oil samples were obtained. The tribological properties of the base oil containing  $\text{Cr}_2\text{AlC}$  were evaluated on a  
UMT-2 ball-on-disc friction and wear tester. The testing of  
20 friction reduction and wear resistance was conducted at rotating speeds of 5 m/min., and loads of 10-30 N for sliding distance  
200m. The material of the upper sample is a 440C stainless steel ball with a diameter of 10mm, hardness of 62 HRC and the  
counterpart is a 45 steel disc of  $\Phi 25\text{mm}\times 5\text{mm}$  in size. The  
25 friction coefficient was recorded automatically with a strain gauge equipped with the tester. The wear scars widths were  
measured by a common optical microscope. Morphologies of friction surfaces were examined using a JSM-5600LV scanning  
electron microscope (SEM). The elements of the friction surface  
30 were analyzed using Energy-dispersive X-ray spectroscopy (EDS).

## 3. Results and Discussion

### 3.1 Phase analysis of $\text{Cr}_2\text{AlC}$

Fig. 1 shows the XRD patterns for blended powders after  
35 magnetic stirred in absolute alcohol, the upper right inset shows the SEM. The main phases of the powders included graphite,  
aluminum and chrome elementary substance, the blended  
powders is small sheet with 10 $\mu\text{m}$ .

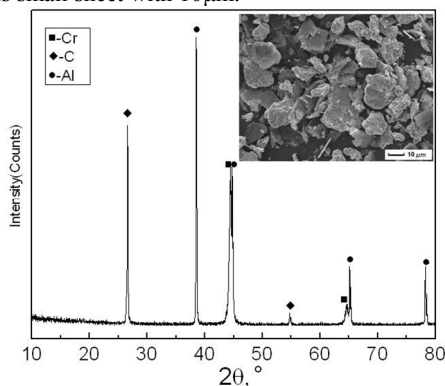
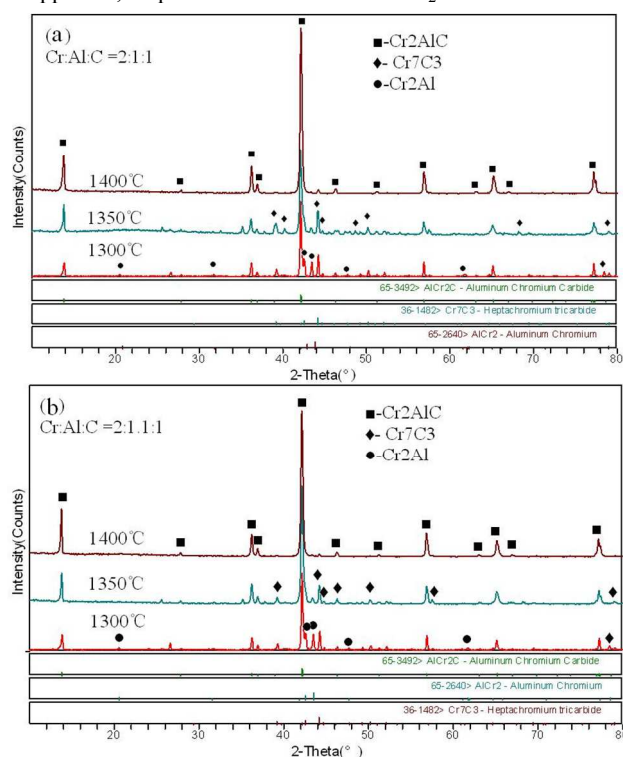


Fig.1 XRD pattern and SEM morphology of blended powders

Fig.2 shows typical XRD patterns of as-synthesized products  
obtained from  $2\text{Cr}/x\text{Al}/\text{C}$  ( $x=1,1.1,1.2$ ) powders mixtures after  
sintered at various temperatures of 1300-1400 °C. It is found that  
all the samples are contained  $\text{Cr}_2\text{AlC}$  phase, the (103) main peak

45 of  $\text{Cr}_2\text{AlC}$  at 42.1° is obvious. When the powder ratio is  
 $2\text{Cr}/1\text{Al}/1\text{C}$  (as shown in Fig.2(a)), for the specimen synthesized  
at 1300 °C,  $\text{Cr}_2\text{AlC}$  was found to be main crystalline phases,  
 $\text{Cr}_2\text{Al}$  and  $\text{Cr}_7\text{C}_3$  were presented as minor phase. As the sintering  
50 temperature was increased to 1350 °C,  $\text{Cr}_2\text{Al}$  phase was gradually  
decreased while the contents of  $\text{Cr}_7\text{C}_3$  and  $\text{Cr}_2\text{AlC}$  phases were  
increased. With further increasing the sintering temperature to  
1400 °C, the  $\text{Cr}_2\text{Al}$  and  $\text{Cr}_7\text{C}_3$  second phases were disappeared,  
major phases were identified as  $\text{Cr}_2\text{AlC}$ . For the specimen  
55 synthesized from  $2\text{Cr}/1.1\text{Al}/1\text{C}$  system shown in Fig.2(b), most  
of the phases synthesized at the temperatures ranged from 1300 to  
1400 °C were similar with those of synthesized from  $2\text{Cr}/1\text{Al}/1\text{C}$   
system, however, contents of  $\text{Cr}_2\text{Al}$  and  $\text{Cr}_7\text{C}_3$  phases were both  
decreased while the intensity of  $\text{Cr}_2\text{AlC}$  peaks are getting  
stronger. As shown in Fig.2(c), with the further addition of Al  
60 into the raw materials, that is  $2\text{Cr}/1.2\text{Al}/1\text{C}$  system,  $\text{Cr}_2\text{Al}$  and  
 $\text{Cr}_7\text{C}_3$  second phases were further decreased, even disappeared at  
the sintering temperature 1300 and 1350 °C, so the  $\text{Cr}_2\text{AlC}$  phase  
was gradually increased, with the specimen synthesized  
temperature high to 1400 °C, the second phases were  
65 disappeared, all phases were identified as  $\text{Cr}_2\text{AlC}$ .



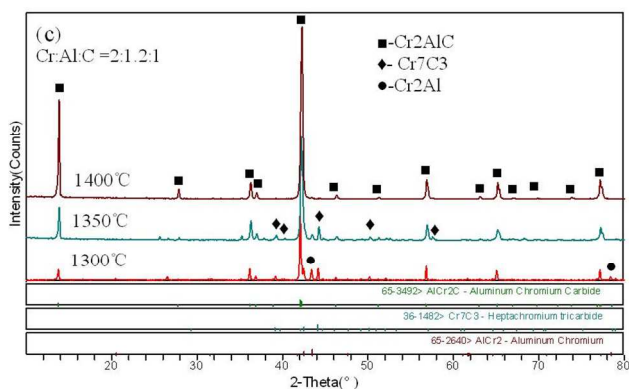


Fig.2 XRD patterns of  $2\text{Cr}/x\text{Al}/\text{C}$  powders after sintered at different temperature with (a)  $x=1$ , (b)  $x=1.1$  and (c)  $x=1.2$ .

As shown in Fig.2, specimen synthesized by pressureless sintering method using Cr, Al and graphite mixed powder as a raw materials at the temperature range of 1300-1400 °C,  $\text{Cr}_2\text{AlC}$  main crystalline phase with small amount of  $\text{Cr}_2\text{Al}$  and  $\text{Cr}_7\text{C}_3$  were identified, also the contents of  $\text{Cr}_2\text{Al}$  and  $\text{Cr}_7\text{C}_3$  second phases were gradually decreased while the intensity of  $\text{Cr}_2\text{AlC}$  peaks are getting stronger with sintering temperature increased. For the specimen synthesized at 1400 °C, high purity  $\text{Cr}_2\text{AlC}$  phase can be synthesized.

Fig.3 shows XRD patterns of the specimen synthesized using the Cr, graphite and different content Al powder mixture by a pressureless sintering at 1400 °C. With the addition of excessive Al into the raw materials, the relative peak intensity of  $\text{Cr}_2\text{AlC}$  obviously increased, which demonstrated that the introduction of excessive Al increased the purity of  $\text{Cr}_2\text{AlC}$  in the products.

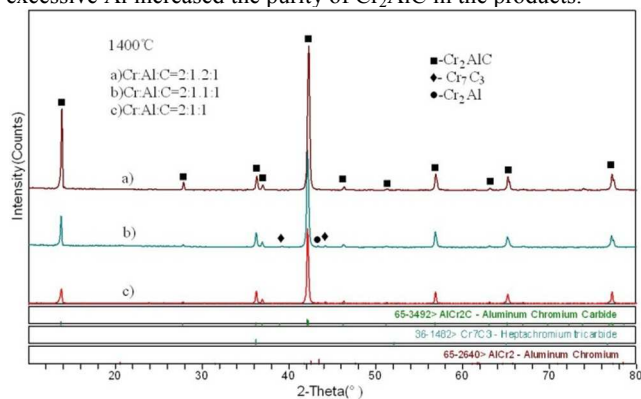


Fig.3 XRD patterns of samples sintered at 1400 °C with different Al content.

### 3.2 Microstructure observation of samples by SEM

Fig.4 shows the SEM images of the synthesized  $\text{Cr}_2\text{AlC}$  powders obtained at 1400 °C. Fig.4 (a) is the micrograph of the sample sintered from powder of  $2\text{Cr}/1\text{Al}/1\text{C}$ , as can be seen from the image, the obtained samples were irregular particles stacked by laminated layers with average size of less than  $5\mu\text{m}$ . Fig.4(b) is enlarged micrograph of Fig.4(a), indicating that the irregular particles are composed of nanoplates with average thickness in the range of 20–30 nm and further confirming the layered nature of the material. Fig.4(c,d) shows the SEM images of the sample sintered from powder of  $2\text{Cr}/1.1\text{Al}/1\text{C}$ . As shown in Fig.4(c), the

sample was composed of a lot of plate-like and block-shaped particles, these particles with different size and smooth surface, further observation shows that the particles have melting imprint, indicating the formation of liquid phase at high temperature. Fig.4 (d) is enlarged SEM image of fractured particles, laminated-like structure of  $\text{Cr}_2\text{AlC}$  is obvious stacked by many uniform nano slices with thickness of about 100 nm, rupture and convolution feature was presented. Fig.4 (e) is SEM images of the sample sintered from powder of  $2\text{Cr}/1.2\text{Al}/1\text{C}$ , in which the particles of this powder are larger, thickness is generally about 50nm. Fig.4 (f) is enlarged SEM image of Fig.4 (e), the growth pattern of laminated-like structure is obviously.

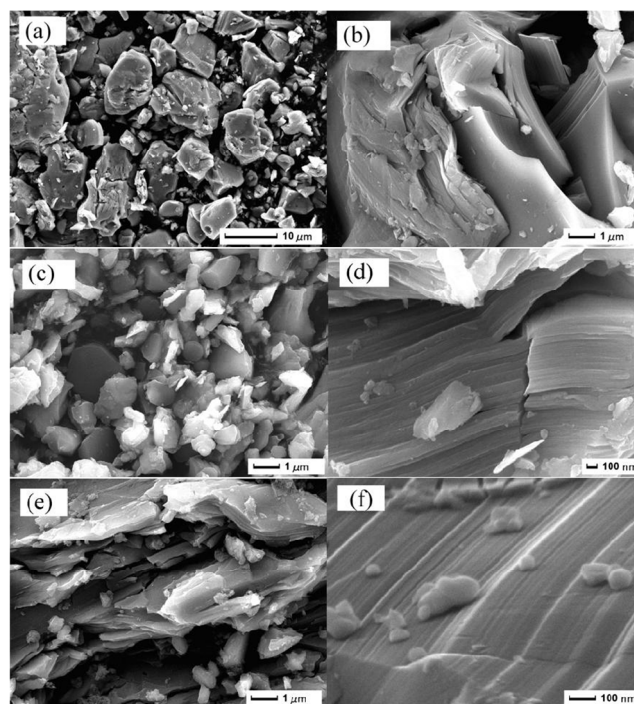


Fig.4 SEM images of the samples sintered at 1400 °C with different Al content.(a) $\text{Cr}:\text{Al}:\text{C}=2:1:1$ ,(b)magnified images of (a), (c)  $\text{Cr}:\text{Al}:\text{C}=2:1.1:1$ , (d)magnified images of (c), (e)  $\text{Cr}:\text{Al}:\text{C}=2:1.2:1$ , (f)magnified images of (e)

### 3.3 Formation process of $\text{Cr}_2\text{AlC}$

In order to understand the formation process of  $\text{Cr}_2\text{AlC}$ , the phase of the sample sintered at different temperatures from 700 °C to 1400 °C using mixed powder of  $2\text{Cr}/1.2\text{Al}/\text{C}$  as starting materials were investigated by XRD technique.

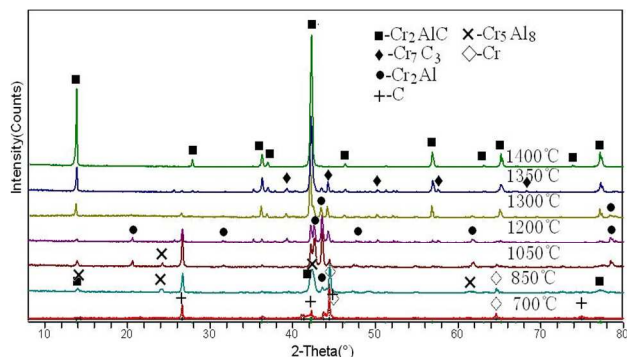


Fig.5 XRD patterns of 2Cr/1.2Al/1C powders sintered at various temperatures.

Fig.5 shows XRD patterns of the powders synthesized under different temperatures. According to Fig.5, C and Cr peaks can be clearly seen in the diffraction profile at 700 °C, peaks at  $2\theta=40$  to  $44^\circ$  appeared broadening that originated from the formation of Cr–Al phases when sintered at 700 °C. For the sample heated to 850 °C and 1050 °C, it can be seen that except for un-reacted C and Cr phases,  $\text{Cr}_2\text{AlC}$  phase has been formed and  $\text{Cr}_5\text{Al}_8$ ,  $\text{Cr}_2\text{Al}$  peaks also can be observed as intermediate phases. With increasing temperature to 1200 °C, C at  $2\theta=26.6^\circ$  and  $\text{Cr}_5\text{Al}_8$  at  $2\theta=24.1^\circ$  peaks abruptly reduced,  $\text{Cr}_2\text{Al}$ ,  $\text{Cr}_7\text{C}_3$  and  $\text{Cr}_2\text{AlC}$  were detected. Except main crystalline phase  $\text{Cr}_2\text{AlC}$ , only quite weak  $\text{Cr}_2\text{Al}$  and  $\text{Cr}_7\text{C}_3$  peak were detected in the sample sintered at 1300 °C. When the temperature was 1350 °C, main crystalline phase  $\text{Cr}_2\text{AlC}$  and a few  $\text{Cr}_7\text{C}_3$  were detected. Further more, when the sintering temperature was as high as 1400 °C, only single-phase  $\text{Cr}_2\text{AlC}$  was detected in the sample. The results indicated that the highly pure  $\text{Cr}_2\text{AlC}$  powder seemed to be easily synthesized by using liquid magnetic stirring and pressureless sintering process from 2Cr/1.2Al/1C powder mixtures.

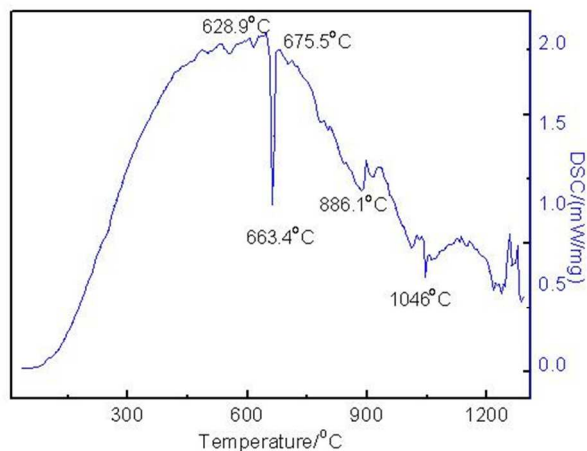


Fig.6 DSC curve of the 2Cr/1.2Al/1C powder mixture at a heating rate of 10 °C/min.

DSC survey was conducted to investigate the formation of products during the sintering process. Typical DSC curve for the blended powders of 2Cr/1.2Al/1C system at a heating rate of 10 °C/min is shown in Fig.6. It can be seen that there is an obvious endothermic peak at 663.4 °C, and there are a lot of endothermic

and exothermic peaks at the temperatures range from 886.1 to 1300 °C, it is sure that the peaks correspond to the frequent reaction and form new compounds. Based on the binary phase diagram of the Cr–Al system,<sup>31</sup> it can be presumed that aluminum melted at 663.4 °C, and reacted with Cr particles to form  $\text{Cr}_x\text{Al}_y$  intermetallics. These endothermic and exothermic peaks at temperatures from 886.1 to 1046.6 °C correspond to the reaction of forming  $\text{Cr}_5\text{Al}_8$  and  $\text{Cr}_2\text{Al}$ . It is considered that the endothermic and exothermic peaks at higher temperatures resulted from the reactions of formation  $\text{Cr}_2\text{AlC}$  and  $\text{Cr}_7\text{C}_3$  by expense of  $\text{Cr}_5\text{Al}_8$ ,  $\text{Cr}_2\text{Al}$  and graphite gradually.

Based on the previous work of  $\text{Cr}_2\text{AlC}$  powder synthesis and the results of this study, the synthesis mechanism of pressureless sintering  $\text{Cr}_2\text{AlC}$  powder was presented. Fig.7 shows the schematic diagram of the synthesized samples obtained by the pressureless sintering process. At the first stage, Al easily melted at 663.4 °C due to its low melting point, and diffusion in the pore of samples, formation molten pool, chromium and graphite was wrapped in the liquid phase of Al. With the sintering temperature increased, chromium and aluminum begins to react in the contact interface, promote formation of chrome aluminum intermetallic. When the sintering temperature increased to 850 °C, the formation of the intermediate phase mainly for the  $\text{Cr}_5\text{Al}_8$  and a small amount of  $\text{Cr}_2\text{Al}$ , at the same time have a small amount of  $\text{Cr}_2\text{AlC}$ , mainly reaction formation by  $\text{Cr}_5\text{Al}_8$ , chromium and graphite, also unreacted Cr and graphite are detected. At a higher temperature of 1050 °C,  $\text{Cr}_5\text{Al}_8$  reaction with the raw material of chromium, aluminum to form  $\text{Cr}_2\text{Al}$ , and at the same time  $\text{Cr}_5\text{Al}_8$ ,  $\text{Cr}_2\text{Al}$  react with graphite to form  $\text{Cr}_2\text{AlC}$ , leading to the reaction product of  $\text{Cr}_5\text{Al}_8$  content decreased,  $\text{Cr}_2\text{Al}$  content increased, chromium and graphite continues to drop,  $\text{Cr}_2\text{AlC}$  continued to rise. When the sintering temperature continues to rise to 1200 °C above, the spawning of  $\text{Cr}_2\text{Al}$  reacted with graphite to form  $\text{Cr}_2\text{AlC}$ , part of chromium reacted with graphite to form  $\text{Cr}_7\text{C}_3$ , as the sintering temperature increased to 1400 °C, the high purity  $\text{Cr}_2\text{AlC}$  is finally fabricated.

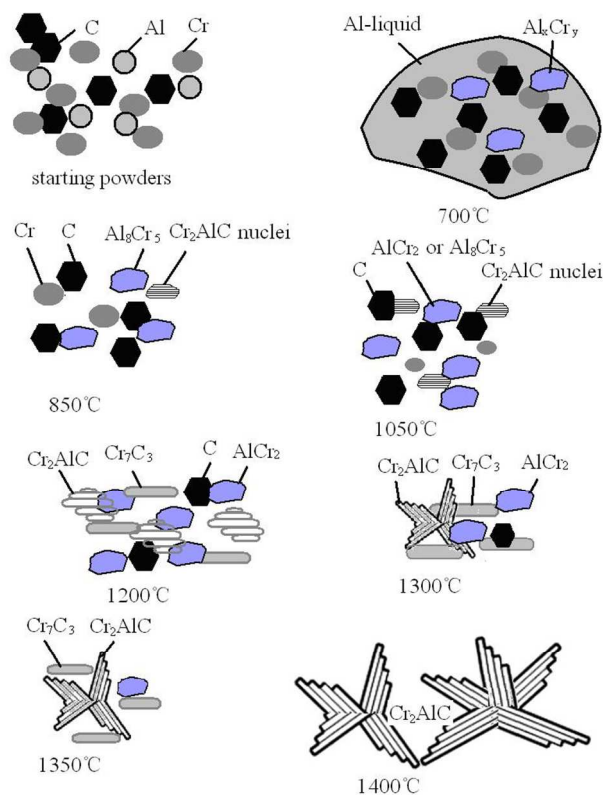


Fig.7 Schematic diagram for the synthesis of  $\text{Cr}_2\text{AlC}$  from the elemental powders.

### 3.4 Friction and wear properties of laminated $\text{Cr}_2\text{AlC}$ crystals

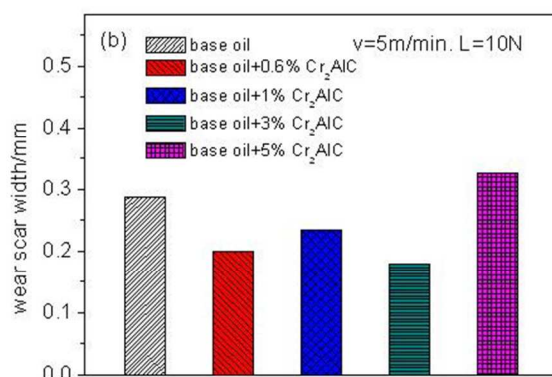
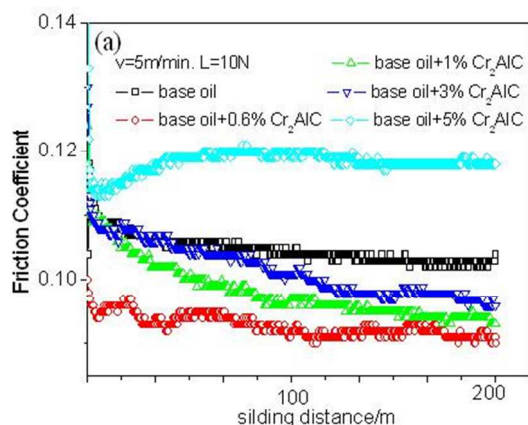


Fig.8 (a) Friction coefficient as a function of sliding distance, (b) wear scar width on disc specimens lubricated with different concentrations  $\text{Cr}_2\text{AlC}$  in 100SN base oil

The tribological behaviors of the as-prepared  $\text{Cr}_2\text{AlC}$  powders as lubrication additive in 100SN base oil were investigated by a UMT-2 ball-on-disc friction and wear tester. Fig.8 (a) shows the friction coefficients vs. sliding distance curves of base oil at 10 N load under 5m/min. sliding speed with different  $\text{Cr}_2\text{AlC}$  concentrations (0-5wt%). It can be observed that the friction coefficient is sensitive to the additive concentration of the laminated  $\text{Cr}_2\text{AlC}$  particles. The friction coefficient of the lubricating system is obviously decreased by adding synthesized laminated  $\text{Cr}_2\text{AlC}$  over a wide concentration range of 0.6–3wt%, the friction coefficients decreased slightly to a steady value with the sliding distance. When the concentration of synthesized laminated  $\text{Cr}_2\text{AlC}$  is 0.6wt%, the best friction coefficient-reducing property is obtained. Contrary to the lower concentrations, the base oil with 5wt% synthesized laminated  $\text{Cr}_2\text{AlC}$  has a relatively higher friction coefficient compared with the base oil. This can be attributed to the fact that the dispersivity of laminated  $\text{Cr}_2\text{AlC}$  is good for 0.6wt% concentration, together with the micro & nano bearing effect, so as to form a layer of tribofilm, and result in a decrease of the friction coefficient.

Fig. 8 (b) gives the wear scar width (WSW) vs. the different  $\text{Cr}_2\text{AlC}$  concentration. It can be seen that the wear scar width of base oil is slight decreased by adding laminated  $\text{Cr}_2\text{AlC}$ , except for the base oil containing 5wt% concentration  $\text{Cr}_2\text{AlC}$  is obviously higher than that of other sample oil, which is in good accordance with the friction coefficient value in Fig.8(a). Therefore, the optimum concentration of the synthesized  $\text{Cr}_2\text{AlC}$  as an additive in base oil is suggested to be 0.6wt%.

In this work, it has been shown that the base oil with a certain viscosity containing 0.6wt%  $\text{Cr}_2\text{AlC}$  can form a certain thickness tribofilm, which can decrease shearing stress, therefore, give a low friction coefficient and wear scar width. In the friction process, because of the contact pressure creating traction-compression stressed zones, a thin tribofilm is formed on the metal substrate, the tribofilm could not only withstand the load of the steel ball but also prevent two mating metal surfaces direct contact.

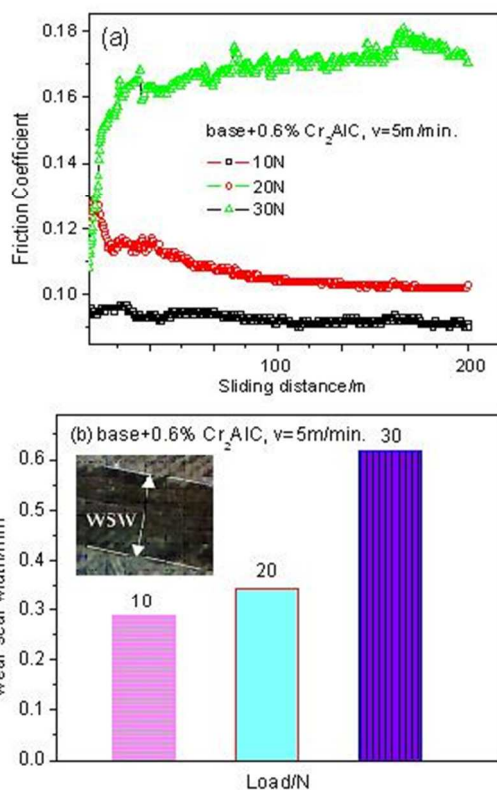


Fig. 9 (a) Friction coefficient, (b) wear scar width of base oil mixed with 0.6% Cr<sub>2</sub>AlC additive under different loads at 5 m/min. for 200m.

Fig.9 (a) show the variation of friction coefficients with sliding distances for 0.6wt% concentration Cr<sub>2</sub>AlC under different loads, respectively. It can be seen that the friction coefficients of base oil with 0.6wt% Cr<sub>2</sub>AlC is stable at about 0.092 under the load of 10N, increasing load to 20N, after an obvious slightly running-in stage, the friction coefficients almost remain constant at about 0.103, the friction coefficient continuously increases along with the sliding distance under the load of 30N.

Fig.9(b) shows the wear scar width (WSW) of 100SN base oil containing 0.6wt% Cr<sub>2</sub>AlC at different loads under a speed of 5 m/min. for 200m. It can be observed that the WSWs increase gradually with the increase of the applied load. The lubrication of Cr<sub>2</sub>AlC as oil additive is mainly dependent on the formation of tribofilm in the friction process. However, a continuous tribofilm only begins to be formed under an optimal load. With further increase of the load, the friction coefficient has increased due to the extrusion of the tribofilm in the contact zone, and result in a high wear scar width.

Fig. 10a displays SEM of the tribofilms formed on the friction surface lubricated by the base oil containing 0.6wt% synthesized laminated Cr<sub>2</sub>AlC. The tribofilms were uniform and tenacious on the friction surface, which results in a lower friction and lower wear scar width. In order to confirm the formation of the tribofilm and its composition, the corresponding EDS analysis of the worn surface was carried out. As shown in Fig. 10b, high intensity peaks from chromium, aluminum, and carbon atoms indicated the formation of an adherent Cr<sub>2</sub>AlC tribofilm. It is believed that the smooth and flat surface lubricated by composites results from the deposition of tribofilm on the friction

surface.

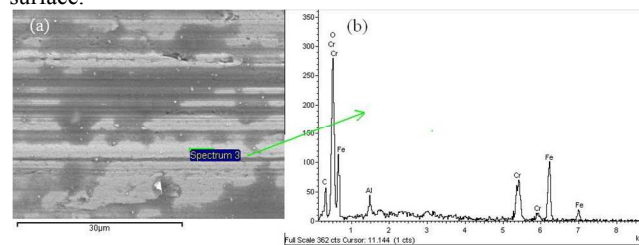


Fig.10 (a) SEM images of the tribofilms formed on the surface (15N, 250r/min., 200m), and (b) EDS spectrum at the surface of point (a).

## 4. Conclusion

By the liquid magnetic stirring mixing raw powders, high purity Cr<sub>2</sub>AlC powder could be pressureless sintering synthesized from Cr, Al and graphite powder at temperature ranged from 1300 to 1400 °C in flowing argon atmosphere. The increase of the Al content in raw materials is helpful to the improvement of Cr<sub>2</sub>AlC phase content, Al element here is considered as a promoting factor because it provides a liquid circumstance to speed up the solid reaction among Cr, Al and graphite. The introduction of 0.6 wt% laminated Cr<sub>2</sub>AlC as lubrication additives improve the tribological properties of the base oil, especially in terms of friction reduction and wear resistance. The excellent tribological properties indicate that the as-prepared Cr<sub>2</sub>AlC will be useful for its further industrial application as oil additive in the future.

## Acknowledgements

This work was supported by the National Natural Science Foundation of China (51275213, 51302112), Jiangsu National Nature Science Foundation (BK2011534), Jiangsu National Nature Science Foundation for Colleges and Universities (14KJB460012), and Scientific and Technological Innovation Plan of Jiangsu Province (CXLX12\_0636).

## Notes and references

- C.Lange, M.Hopfeld and M.W.Barsoum, *Phys. Status. Solidi. A*, 2012, **209**, 545.
- M.W. Barsoum, *J Prog. Solid State Chem.*, 2000, **28**, 201.
- Z.M. Sun, *Int. Mater. Rev.*, 2011, **56**, 143.
- S.B. Li, H.L. Li and Y. Zhou, *J. Eur. Ceram. Soc.*, 2014, **34**, 1083.
- M. Xue, H. Tang and C.S. Li, *Adv. Appl. Ceram.*, 2014, **113**, 245.
- D. Li, Y. Liang and X.X. Liu, *J. Eur. Ceram. Soc.*, 2010, **30**, 3227.
- X.H. Wang, Y.C. Zhou, *J. Mater. Chem.*, 2002, **12**, 2781.
- W.B. Tian, P.L. Wang and G. Zhang, *Mater. Sci. Eng. A*, 2007, **454**, 132.
- L.O. Xiao, S.B. Li and G.M. Song, *J. Eur. Ceram. Soc.*, 2011, **31**, 1497.
- J.D. Hettinger, S.E. Lofland and P. Finkel, *Phys. Rev. B*, 2005, **72**, 115.
- T.H. Scabarozzi, S. Amini and O. Leafner, *J. Appl. Phys.*, 2009, **105**, 013543-013543.
- J. Wang, Y. Zhou, *Annu. Rev. Mater. Res.*, 2009, **39**, 415.
- W.B. Tian, P.L. Wang and Y.M. Kan, *J. Mater. Sci.*, 2008, **43**, 2785.
- Z.J. Lin, M.S. Li and J.Y. Wang, *Acta. Mater.*, 2007, **55**, 6182.
- Y.L. Du, Z.M. Sun and H. Hashimoto, *J. Appl. Phys.*, 2011, **109**, 063707.
- W.B. Tian, P.L. Wang and G. Zhang, *Scripta. Mater.*, 2006, **54**, 841.
- W.B. Tian, P.L. Wang and G. Zhang, *J. Am. Ceram. Soc.*, 2007, **90**, 1663.
- C. Hu, L. He and J. Zhang, *J. Eur. Ceram. Soc.*, 2008, **28**, 1679.
- S.B. Li, W.B. Yu and H.X. Zhai, *J. Eur. Ceram. Soc.*, 2011, **31**, 217.

- 
- 20 B. Manoun, R. Rgolve and S.K. Saxena, *Phys. Rev. B*, 2006, **73**,1.  
21 D.B. Lee, T.D. Nguyen, *J. Alloys. Compd.*, 2008, **464**,434.  
22 W.B.Tian, K. Vanmeensel and P.L.Wang, *Mater. Lett.*, 2007, **61**, 4442.  
23 W.B. Zhou, B.C. Mei and J.Q. Zhu, *J. Mater. Sci.*, 2005, **40**,3559.  
5 24 S. Amini, A.G. Zhou and S. Gupta, *J. Mater. Res.*, 2008, **23**,2157.  
25 W.B. Tian, Z.M. Sun and Y.L. Du, *Mater. Lett.*, 2008, **62**,3852.  
26 Q. Wu, C.S. Li and H. Tang, *Appl. Surf. Sci.*, 2010, **256**,6986.  
27 M.A. Elsaied, F.A. Deorsola and R.M. Rashad, *Int. J. Refract. Met. Hard. Mater.*, 2012, **35**,127.  
10 28 S. Gupta, D. Filimonov and T. Palanisamy, *Wear*, 2008, **265**,560.  
29 D. Filimonov, S. Gupta and T. Palanisamy, *Tribol. Lett.*, 2009, **33**,9.  
30 S. Gupta, D. Filimonov and V. Zaitsev, *Wear*, 2008, **264**,270.  
31 W.B. Tian, P.L.Wang and Y.M.Kan, *Mater. Sci. Eng. A*, 2007, **443**,229.

15